PHYSICAL REVIEW E VOLUME 59, NUMBER 3 MARCH 1999

Curvature distributions of spinodal interface in a condensed matter system

Hiroshi Jinnai,[1,*] Yukihiro Nishikawa,[1] and Takeji Hashimoto[1,2,†]
[1]*Hashimoto Polymer Phasing Project, ERATO, Japan Science and Technology Corporation, 15 Morimoto-cho, Shimogamo, Sakyo-ku, Kyoto 606-0805, Japan*
[2]*Department of Polymer Chemistry, Graduate School of Engineering, Kyoto University, Kyoto 606-8501, Japan*
(Received 15 December 1998)

The time evolution of a three-dimensional spatially bicontinuous interface of a phase-separated polymer blend, as a model of condensed matter systems, in late stage spinodal decomposition (SD) has been studied by laser scanning confocal microscopy. Probability densities of the mean and the Gaussian curvatures of the interface have been obtained. The probability densities of the curvatures at various times were successfully scaled by a characteristic length, which confirms the validity of the dynamical scaling law. We found that a large portion of the interface formed in late stage SD consists of saddle-shaped surfaces.
[S1063-651X(99)51003-9]

PACS number(s): 83.80.Es, 64.70.Ja, 64.75.+g, 83.70.Hq

If a mixture is quenched from the single phase region to the spinodal region of the phase diagram by changing thermodynamic variables such as temperature, it becomes thermodynamically unstable and separates, via spinodal decomposition (SD), into two phases [1–3]. A bicontinuous two-phase structure appears during SD if the volume fraction of one of the phases is close to 0.5 (''isometric''). Such bicontinuous structures are commonly formed in a variety of condensed atomic and molecular systems, e.g., in binary mixtures of polymers [3], simple liquids [4–6] as well as metallic alloys [7,8], microemulsions [9] and inorganic glasses [10]. Universality of the SD behavior among these systems can be found [11].

In late stage SD, the compositions of two coexisting phases have already reached equilibrium, and the excess free energy of the system, now localized at the interface between the two phases, decreases with time *t*. Therefore, under such conditions, the most significant physical parameters are the interface curvatures (i.e., the mean and the Gaussian curvatures), which determine the interface dynamics [12]. Except for a few cases, to our knowledge, no quantitative evaluation of the interface curvatures has been done [13,14]. This is due to experimental difficulties in taking real space images of complex structures, e.g., bicontinuous structures, in three dimensions (3D). However, the 3D images should capture the local structure of the interface, as well as its global topology. Thus, they are of central importance to the physics of the system undergoing late stage SD. We note that 3D real space measurements for an off-critical mixture, which exhibit minority phase droplets inside a matrix of the majority phase and hence show much simpler morphologies than the bicontinuous structure, have only been recently done. The time evolution of distribution of droplet domain sizes was examined to study the coarsening dynamics [15].

The mixtures studied consisted of deuterated polybutadiene (DPB) and polybutadiene (PB). The weight-average molecular weight (M_w) and polydispersity (M_w/M_n) of the DPB were, respectively, 143×10^3 and 1.12 (M_n denotes the number-average molecular weight). M_w and M_w/M_n for the PB were 95×10^3 and 1.07, respectively. A small amount of anthracene was attached to the PB for contrast enhancement of the microscopy [16]. The DPB/PB blend exhibits an upper critical solution temperature type phase diagram with the critical composition of the DPB as 46 vol % according to the Flory-Huggins lattice theory [17]. The spinodal temperature at the critical composition was estimated to be ca. 110 °C [16]. A critical mixture of DPB and PB was dissolved in benzene to form ca. a 7 wt % solution and then lyophilized. The mixture after lyophilization was homogenized by mechanical mixing [18] and placed between cover slips. The mixture was annealed at 40 °C for six different t (t=1350, 1675, 2880, 4610, 7365, and 8610 min), all characteristics of late stage SD. The mixtures were subsequently observed by laser scanning confocal microscopy (LSCM) (Carl Zeiss, LSM410™) with a 364-nm laser at room temperature.

Oil-immersed 40× (Plan-Neofluar, Carl-Zeiss) objective with a numerical aperture of 1.3 was used to record sliced images at 0.5-μm increments along the optical axis of the microscope (the z axis) perpendicular to the focal plane (the lateral plane). The lateral and axial resolutions were approximately 0.24 μm and 0.92 μm, respectively. The raw images were subjected to the image processing and then ''binarized'' with an appropriate threshold [11,16]. The interface between the DPB and PB components was modeled using contiguous polygons [19]. We note that the volume fraction of DPB was time independent, i.e., 0.5 ± 0.02 over the whole experimental time range.

The structure factor, $S(q,t)$, is obtained from the following relations: $S(q,t)\sim|A(q,t)|^2$ and $A(q,t)\sim\mathcal{F}(C(r,t))$, where $A(q,t)$ and $C(\mathbf{r},t)$ represent the structure amplitude and spatial distribution of the (binarized) image contrast where PB=1 and DPB=0 in 3D. $\mathcal{F}(f(\mathbf{r}))$ denotes the Fourier transformation of $f(\mathbf{r})$. The wave number is defined as $q=2\pi j/NL$ ($j=0,1,2,...,N/2$; N and L are number of pixels along the edge of the image and the size of the square pixel, respectively). The scaled structure factor, $S_{\mathrm{LSCM}}(x,t)\equiv q_m(t)^3S(x,t)$($x\equiv q/q_m(t)$), at various t became a time-independent function, demonstrating that the dynamical scaling law holds in late stage SD process in the DPB/PB mixture. We have com-

*Electronic address: hjinnai@ipc.kit.ac.jp
†Electronic address: hashimoto@alloy.polym.kyoto-u.ac.jp

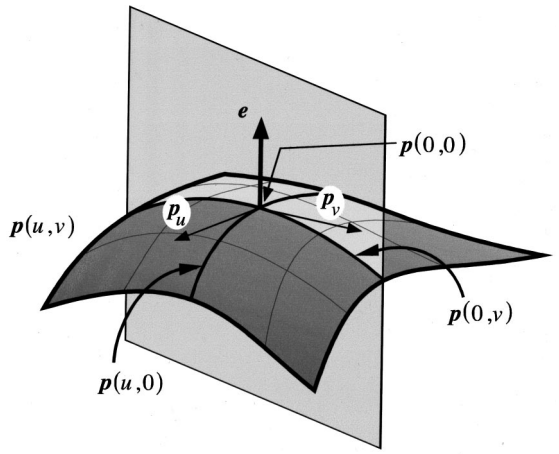

FIG. 1. Schematic diagram of a surface expressed in a parametric form $\mathbf{p}(u,v)$ and a ''sectioning plane,'' which is comprised of $\mathbf{e}$ and $\mathbf{p}(0,v)$. $\mathbf{p}(0,0)$ is a point of interest at which the local curvatures are measured.

pared $S_{\mathrm{LSCM}}(x,t)$ with that obtained independently from light scattering (LS) experiments on the DPB/PB mixture in late stage SD, $S_{\mathrm{LS}}(x,t)$; they were in excellent quantitative agreement, suggesting that the 3D structure reflects a real structural entity. Moreover, $S_{\mathrm{TDGL}}(x,t)$ obtained from a computer simulation on the basis of the time-dependent Ginzburg-Landau (TDGL) theory with hydrodynamic interactions [12,20], quantitatively accounts for both $S_{\mathrm{LSCM}}(x,t)$ and $S_{\mathrm{LS}}(x,t)$. It is important to note that $S_{\mathrm{TDGL}}(x,t)$ represents the structure factors of various binary systems, including polymers [21] and simple liquids [5].

Some wave numbers characteristic to the evolving bicontinuous structure were estimated from the 3D LSCM images. The wave number at the maximum intensity of $S(q,t)$, $q_m(t)$, which relates to the characteristic wavelength, $\Lambda_m(t)$, by $\Lambda_m(t)=2\pi/q_m(t)$. We found $q_m(t) \sim t^{-1}$. Another wave number, the interface area per unit volume, $\Sigma(t)$, can also be obtained from LSCM images. $\Sigma(t) \sim t^{-1}$ was found. A scaled length parameter, $\Sigma(t)q_m(t)^{-1}$, turned out to be time independent. The plateau value was 0.44, while the TDGL predicted a value of 0.5 [21]. All of those results are consistent with the predictions from the TDGL simulation [12,20].

The 3D interface developed in late stage SD (''spinodal interface'') was then subjected to an analysis for probability densities of the curvatures [22]. In Fig. 1, the surface is expressed in a parametric form as $\mathbf{p}(u,v)$ around a point of interest (POI) at which the curvatures are measured. The coordinate (u,v) is arbitrarily set on the surface and the POI is expressed as $(u,v)=(0,0)$. The first and second fundamental forms in differential geometry are expressed as [23]

$$I = E\,du\,du + 2F\,du\,dv + G\,dv\,dv, \tag{1a}$$

and

$$II = L\,du\,du + 2M\,du\,dv + N\,dv\,dv. \tag{1b}$$

The parameters in Eqs. (1a) and (1b) are given by

$$E=\mathbf{p_u}\cdot\mathbf{p_u}, \quad F=\mathbf{p_u}\cdot\mathbf{p_v}, \quad G=\mathbf{p_v}\cdot\mathbf{p_v},$$

$$L=\mathbf{p_{uu}}\cdot\mathbf{e}, \quad M=\mathbf{p_{uv}}\cdot\mathbf{e}, \quad N=\mathbf{p_{vv}}\cdot\mathbf{e}, \tag{2}$$

where $\mathbf{e}$ is a unit vector normal to the surface at the POI, defined by $\mathbf{e}=\mathbf{p_u}\times\mathbf{p_v}/|\mathbf{p_u}\times\mathbf{p_v}|$ and the subscripts of $\mathbf{p}$ represent the partial derivatives, i.e., $\mathbf{p_u}=\partial\mathbf{p}/\partial u$ and $\mathbf{p_{uv}}=\partial^2\mathbf{p}/\partial u\,\partial v$. The mean, H, and the Gaussian, K, curvatures can be expressed in terms of the above parameters:

$$H=\frac{1}{2}(\kappa_1+\kappa_2)=\frac{EN+GL-2FM}{2(EG-F^2)}, \qquad K=\kappa_1\kappa_2=\frac{LN-M^2}{EG-F^2}. \tag{3}$$

κ_1 and κ_2 are the principal curvatures at the POI. The surface is first ''sectioned'' by a plane that contains $\mathbf{p_u}$ and $\mathbf{e}$. The intersection between the plane and the surface is defined as $\mathbf{p}(u,0)$. Parameters E and L in Eq. (2) can be obtained from $\mathbf{p}(u,0)$. The surface is then cut by another plane that defines $\mathbf{p}(0,v)$. Now F, G, and N can be computed. The parameter M remains unsolved since it needs complete functional form, i.e., $\mathbf{p}(u,v)$. Determining this was difficult. Thus, we rearranged Eqs. (2) and (3) to eliminate M,

$$f(i,H,K)\equiv 0 = 4F_i^2\left\{L_iN_i-K(E_iG_i-F_i^2)\right\} - \left\{E_iN_i+G_iL_i-2H(E_iG_i-F_i^2)\right\}^2. \tag{4}$$

Here the subscript i denotes ith set of the curvilinear coordinates (u,v) defined by the two sectioning planes. Since two unknown quantities, H and K, are invariant for any choice of the coordinates, in principle, Eq. (4) with two sets of the curvilinear coordinates gives the simultaneous equation for H and K. In reality, several sets of $f(i,H,K)$ are obtained at the POI, from which the curvatures are evaluated by using nonlinear regression fitting [sectioning and fitting method (SFM)] [22].

Since the SFM provides local surface curvatures at a given point on the surface, the joint probability density, $P(H,K;t)$, at a given t can be obtained by sampling ca. 200×10^3 surface points randomly chosen. Typically, the entire surface consists of about 2×10^6 surface points. We made sure that the number of points used for determining $P(H,K;t)$ are enough so that the shape of the distribution becomes invariant with further sampling. $\int\int P(H,K;t)dH\,dK=1$ was used for normalization. Figure 2 shows $P(H,K;t)$ at $t=1675$ min, which has a characteristic functional form, elucidating the following characteristics: (i) Most of the measured points (up to 93%) lie in the $K<0$ region, demonstrating that the interface is anticlastic. Namely, two principal curvatures have opposite signs at a large portion of the interface. (ii) The probability for $K>0$, corresponding to the synclastic surface, is small. (iii) The observed probability density fulfills a relation of $K\leqslant H^2$. This relation is required because the principal curvatures, which can be calculated from H and K via $\kappa_i=H\pm\sqrt{H^2-K}$ $(i=1,2)$, should be real numbers.

From $P(H,K;t)$, the probability densities of the mean curvature, $P_H(H;t)$, and that of the Gaussian curvature, $P_K(K;t)$ are calculated from

$$P_H(H;t)\equiv\int P(H,K;t)dK,$$

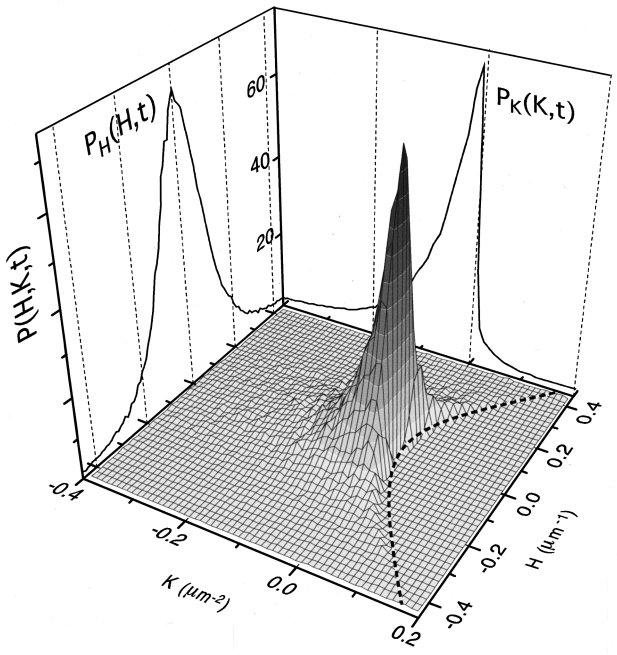

FIG. 2. Bird's-eye view of the joint probability density *P(H,K;t)* for the DPB/PB mixture at $t=1675$ min. $P_H(H;t)$ and $P_K(K;t)$ are also shown. The broken parabolic line shows $K=H^2$.

and

$$P_K(K;t) \equiv \int P(H,K;t)\,dH. \tag{5}$$

Figure 3 demonstrates the time evolution of the probability densities. $P_H(H;t)$ is symmetric about $H=0$ and thus the area-averaged H stayed close to zero [see Fig. 3(a)], implying that the system tends to take most reasonable evolution

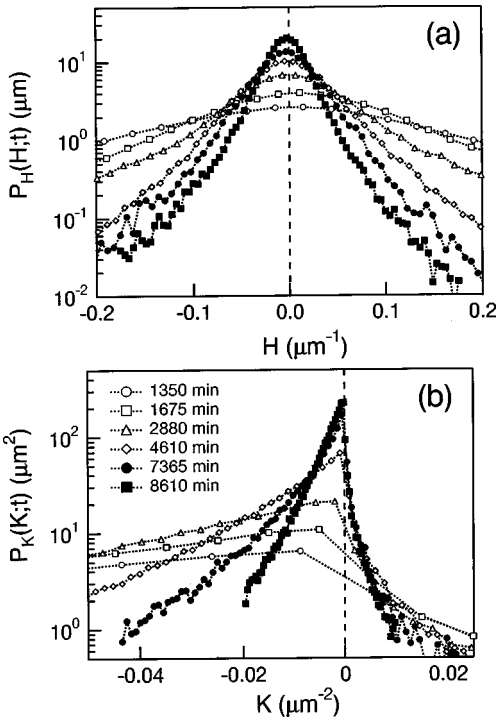

FIG. 3. Time-evolution of (a) $P_H(H;t)$ and (b) $P_K(K;t)$ for the DPB/PB mixture in late stage SD.

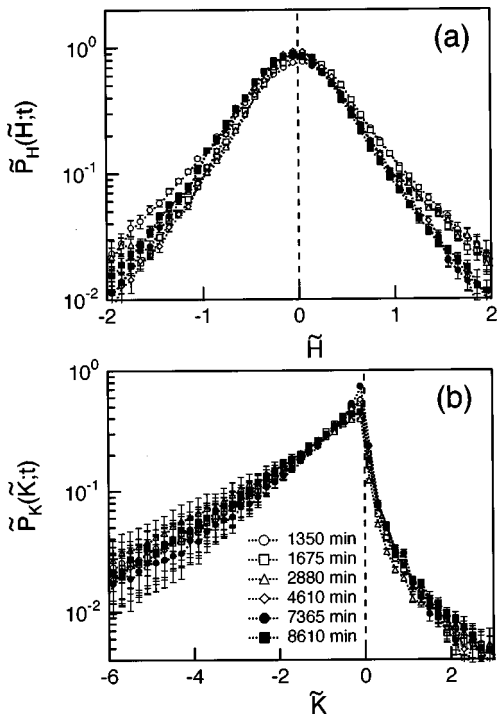

FIG. 4. Scaled probability densities (a) $\tilde{P}_H(\tilde{H};t)$ and (b) $\tilde{P}_K(\tilde{K};t)$ for the DPB/PB mixture in late stage SD.

path with a low free energy in the SD process. $P_K(K;t)$ is distributed mostly in the $K<0$ region, demonstrating that the interface is hyperbolic regardless of *t.* The full width at half maximum of $P_H(H;t)$ decreased, thus the portion of the distribution with small $|H|$ increased with *t.* Similarly, the portion of small $|K|$ increases as time elapsed [14]. These results suggest that the average radius of curvature of the spinodal interface increased, i.e., the interface became smoother with *t.*

In order to show the dynamical scaling law for the local structure, such as the probability densities of the curvatures, we used the inverse of $\Sigma(t)$ for a length characteristic to the bicontinuous structures. The scaled probability densities of H, $\tilde{P}_H(\tilde{H};t)$, and K, $\tilde{P}_K(\tilde{K};t)$, are respectively obtained by $\tilde{P}_H(\tilde{H};t)=\Sigma(t)P_H(H;t)$ and $\tilde{P}_K(\tilde{K};t)=\Sigma(t)^2P_K(K;t)$. Here $\tilde{H}=H\Sigma(t)^{-1}$ and $\tilde{K}=K\Sigma(t)^{-2}$. The scaled probability densities are plotted against t in Fig. 4, demonstrating that the dynamical scaling law holds for the probability densities of curvatures within experimental accuracy as well as for the scattering structure factor. Note that the examination of the dynamical scaling through *S(x,t)* has been done many times; most of the studies showed the self-similar growth of the global structure, which is characterized by the scattering maximum, i.e., a structure corresponding to the length scale of $\Lambda_m(t)$. Although the curvatures and *S(q,t)* are implicitly related to each other, a general relationship between them is not at all clear. Hence, it is impossible to discuss whether or not the local shape of the interface really follows the dynamical scaling law from the scattering data. Meanwhile, the curvatures presented in the present study qualify the local shape of the structure. Thus, the results shown in Fig. 4 stand out from the fact that they demonstrate that not only the global structure but also the local shape of the spinodal interface evolves with the dynamical self-similarity. In addi-

tion, the probability densities experimentally obtained in the present study are expected to be universal in a variety of condensed matter systems.

Information about the time evolution of the curvatures should be useful in predicting interface dynamics and interface stability [12], especially in late SD. For example, one would study how a particular part of the interface would change its shape during SD by examining the time change of the interface curvatures. Knowledge of such interface movement should be essential to understand the mechanism of the SD process. Such analysis is under progress [16].

In summary, the probability densities of the curvatures of the interface in a phase-separated bicontinuous structure have been measured. We found that the large portion of the interface is anticlastic and the mean curvature is symmetrically distributed around $H=0$. The probability densities of the curvatures at various times were found to be scaled by a characteristic wave number, i.e., the interface area per unit volume in late stage SD. This demonstrates that the dynamical scaling holds for the probability densities of the curvatures as well.

We would like to thank Dr. Tsuyoshi Koga and Dr. Stephen T. Hyde for their stimulating discussions. Thanks are due to Dr. Alan I. Nakatani for reading the entire text in its original form.

[1] J. D. Gunton, M. San Miguel, and P. S. Sahni, in *Phase Transition and Critical Phenomena*, edited by C. Domb and J. L. Lebowitz (Academic, New York, 1983), Vol. 8, p. 269.

[2] K. Binder, in *Materials Science and Technology: A Comprehensive Treatment*, edited by R. W. Cahn, P. Haasen, and E. J. Kramer (VCH, Weinheim, 1990), Vol. 5, p. 405.

[3] T. Hashimoto, in *Materials Science and Technology*, edited by R. W. Cahn, P. Haasen, and E. J. Kramer (VCH, Weinheim, 1993), Vol. 12, p. 251.

[4] J. S. Hung, W. I. Goldburg, and A. W. Bjerkaas, Phys. Rev. Lett. **32**, 921 (1974).

[5] Y. Chou and W. I. Goldburg, Phys. Rev. A **20**, 2105 (1979).

[6] C. M. Knobler and N.-C. Wong, J. Phys. Chem. **85**, 1972 (1981).

[7] S. Komura and H. Furukawa, *Dynamics of Ordering Processes in Condensed Matter* (Plenum, New York, 1998).

[8] S. Komura, Phase Transit. **12**, 3 (1988).

[9] F. Mallamace, N. Micali, S. Trusso, and S.-H. Chen, Phys. Rev. E **51**, 5818 (1995).

[10] A. Craievich and J. M. Sanchez, Phys. Rev. Lett. **47**, 1308 (1981).

[11] T. Hashimoto, T. Koga, H. Jinnai, and Y. Nishikawa, Nuovo Cimento D (to be published).

[12] K. Kawasaki and T. Ohta, Physica A **118**, 175 (1983).

[13] T. Kawakatsu, K. Kawasaki, M. Furusaka, H. Okabayashi, and T. Kanaya, J. Chem. Phys. **99**, 8200 (1993).

[14] H. Jinnai, T. Koga, Y. Nishikawa, T. Hashimoto, and S. T. Hyde, Phys. Rev. Lett. **78**, 2248 (1997).

[15] W. R. White and P. Wiltzius, Phys. Rev. Lett. **75**, 3012 (1995).

[16] H. Jinnai, Y. Nishikawa, H. Morimoto, and T. Hashimoto, Macromolecules (to be published).

[17] P. J. Flory, *Principles of Polymer Chemistry* (Cornell University Press, New York, 1953).

[18] T. Hashimoto, T. Izumitani, and M. Takenaka, Macromolecules **22**, 2293 (1989).

[19] Y. Nishikawa, H. Jinnai, T. Koga, T. Hashimoto, and S. T. Hyde, Langmuir **14**, 1242 (1998).

[20] T. Koga and K. Kawasaki, Phys. Rev. A **44**, R817 (1991).

[21] T. Koga, K. Kawasaki, M. Takenaka, and T. Hashimoto, Physica A **198**, 473 (1993).

[22] Y. Nishikawa, T. Koga, H. Jinnai, and T. Hashimoto (unpublished).

[23] D. Hilbert and S. Cohn-Vossen, *Geometry and the Imagination* (Chelsea Publishers, New York, 1952).